A GENERALIZED FRAMEWORK TO TRANSPORT GEOPHYSICAL FIELDS: A DIFFERENTIAL GEOMETRY PERSPECTIVE

A PREPRINT

Yicun Zhen[1], Valentin Resseguier[2,3], and Bertrand Chapron[4]

[1]Department of Oceanography, Hohai University, Nanjing, Jiangsu, China
[2]LAB, SCALIAN DS, Rennes, France
[3]INRAE, OPAALE, Rennes, France
[4]Laboratoire d'Océanographie Physique et Spatiale, Ifremer, Plouzané, France

December 8, 2023

ABSTRACT

To estimate displacements of physical fields, a general framework is proposed. Considering that for each state variable, a tensor field can be associated, ways these displacements act on different state variables will differ according to the tensor field definitions. This perspective provides a differential-geometry-based reformulation of the generalized optical flow (OF) algorithm. Using the proposed framework, optimisation procedures can explicitly ensure the conservation of certain physical quantities (total mass, total vorticity, total kinetic energy, etc.). Existence and uniqueness of the solutions to the local optimisation problem are demonstrated, leading to a new nudging strategy using all-available observations to infer displacements of both observed and unobserved state variables. Using the proposed nudging method before EnKF, numerical results show that ensemble data assimilation better preserves the intrinsic structure of underline physical processes if the ensemble members are aligned with the observations.

1 Introduction

Since chaotic divergence is an intrinsic property of turbulent geophysical systems, data assimilation is often necessary to improve model trajectories of state variables. Numerous strategies have then been proposed, including nudging methods, 3-Dimensional variational method [17], Kalman filter based methods [13][14][19][15], 4-Dimensional variational methods [6], and particle filters [7].

If $x^b(t)$ denotes the state vector at time t estimated by the model, and $y^o(t)$ the observed state variables at the same time t, a first step is to quantify differences between $x^b(t)$ and $y^o(t)$. Different interpretations of this space of errors result in different data assimilation algorithms. For illustration, consider x^b and y^o, Fig. 1. The difference simply relates to shifted positions of two bright spots. Numerically $y^o - x^b$ can possibly result in two different nudging strategies :

Strategy 1 (nonlinear): $x^b(x) \longleftarrow x^b(x - \epsilon v(x))$;

Strategy 2 (linear): $x^b(x) \longleftarrow (1-\epsilon)x^b(x) + \epsilon y^o(x)$,

where $v(x)$ is a vector field determined by y^o and x^b, encoding the displacement of each point in the domain. The linear strategy is the most commonly used nudging strategy. However, a nonlinear nudging strategy seems more natural. It can preserve the main physical feature of the physical field, e.g. bright spots for this example, during the whole nudging process. In general, a position error can be represented by an invertible smooth map $T : \Omega \longrightarrow \Omega$ to represent the displacement of each point in the domain Ω.

*Corresponding author: zhenyicun@proton.me

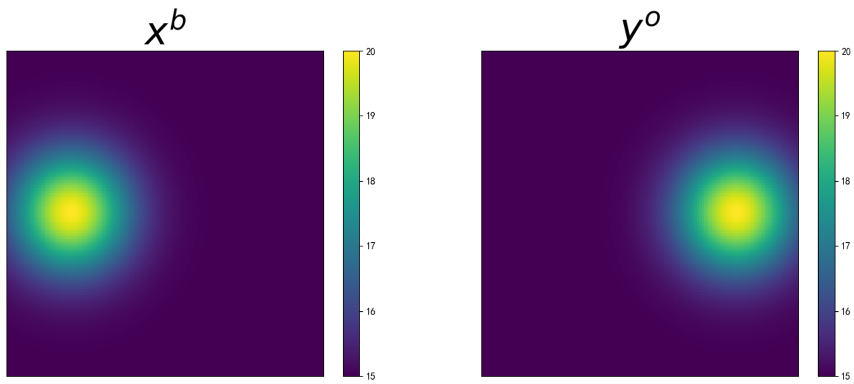

Figure 1: Suppose that the difference between the model estimate x^b and observed state y^o only differ by the position, then apparently a nudging strategy that gradually moves x^b rightward is more reasonable than the linear nudging strategy.

A numerical evaluation of T for two physical fields S_1 and S_2, can then target the minimization of a cost function of the following form:

$$\begin{cases} T = \underset{T\in C^\infty_{\text{inv}}(\Omega,\Omega)}{\arg\min} \|S_1 - T^\# S_2\|^2 + a\|T\|^2 \\ \text{Proper boundary conditions} \end{cases} \tag{1}$$

in which $C^\infty_{\text{inv}}(\Omega,\Omega)$ refers to the set of smooth 1-1 and onto maps from Ω to itself. $T^\# S_2$ represents how S_2 transforms under the map T. $\|T\|$, a chosen norm for the map T, serves as a regularization term. $a > 0$ is a pre-chosen positive constant that weights this regularization term. Directly solving the optimisation problem (1) may technically be too difficult. Instead, it might be easier to iteratively solve an "infinitesimal" version :

$$\begin{cases} v_i = \underset{\mathbf{v}:\Omega\to\mathbb{R}^n}{\arg\min} \dfrac{\partial\|S_1 - (Id + sv)^\# S_2\|^2}{\partial s}\Big|_{s=0} + a\|v\|^2 \\ \text{Proper boundary condition for } v_i, \end{cases} \tag{2}$$

where v_i is the vector field at the $i-$th iterative step, Id the identity map on Ω. For each i, v_i is the "optimal" vector field along which S_2 the most fast transforms towards S_1. At each iterative step, S_2 is replaced with $(Id + \epsilon v_i)^\# S_2$ for some pre-chosen small ϵ. Iteratively solving (2) results in a displacement flow Φ:

$$\frac{\partial\Phi(s,x)}{\partial s}\Big|_{s=k\epsilon} = v_k(\Phi(k\epsilon, x)). \tag{3}$$

And the displacement map $T(x) = \Phi(N\epsilon, x) \approx (Id+\epsilon v_N)\circ\cdots\circ(Id+\epsilon v_1)$ is our candidate solution for (1). However, not every smooth 1-1 and onto map T can be approximated by a sequential composition of small displacements. Therefore the optimisation problems (1) and (2) can be fundamentally different. Our present motivation is on a reformulation and solution of (2).

A key is to design a method to include the definition of $T^\#$ and the choice of norms for the two terms in Eq.(2). The definition of $T^\#$ is essential and some relevant algorithms are reviewed or briefly discussed in section 2 and section 3, including the optical flow (OF) algorithms [1, 29, 16], the large deformation diffeomorphisms [26, 23, 3, 4], the metamorphoses strategy [25, 24], and some other algorithms [20, 2]. Although some of these algorithms have been widely applied to geophysical observations, $T^\#$ are commonly used without considering the dynamics of the geophysical fields. The displacement map T may then cause severe structural errors when applied to unobserved state variables. Fig.2 illustrates an example of directly applying T by composition. The original physical field S is a rotational vector field, rotating counter-clockwise. Suppose that a displacement map T is to be estimated from observations of other state variables. T is assumed to be a clockwise rotation by $90°$. A direct application of T then transforms S to a displacement field $S \circ T^{-1}$ displaying completely different features.

To circumvent such undesirable results, [30] considered a differential geometry framework and the use of tensor fields to formulate $T^\#$ in Eq.(1) and (2). In this new perspective, the choice of tensor fields can then be explicitly dictated by the dynamical equations of the underline physical fields. $T^\#$ will follow dynamical principles, and certain

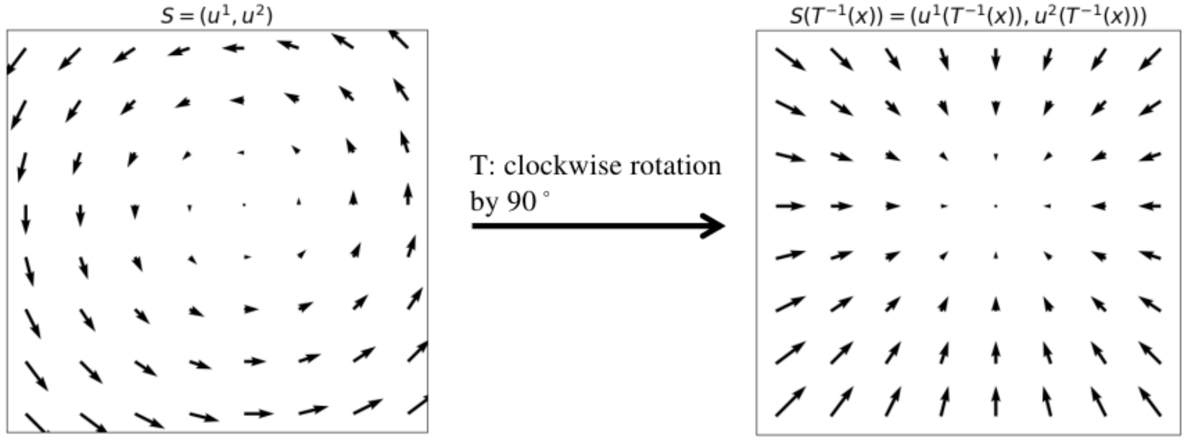

Figure 2: Suppose that the original field S is a rotating wind field and the given displacement map T is clockwise rotation by $90°$. Then the direct composition of S and T results in a wind field of completely different feature.

physical quantities are naturally conserved during the morphing process. A similar argument has been given for small displacement cases [28]. This further leads to a new alignment strategy in which the displacement flow calculated from the observed state variables can also be applied to partially correct the displacement of the physical fields of unobserved state variables. Such a new alignment strategy can naturally be incorporated with the classical ensemble Kalman filter to reduce inherent difficulties arising from linear algorithms.

The constrained formulation of $T^{\#}$, based on the concept of tensor fields is given in section 2. This leads to a new version of the optimisation problem in the form of (2). Existence and uniqueness of the resulting solution are provided. A physical interpretation of the new optimisation problem is discussed, with a brief review of some classical OF algorithms [1, 29, 16]. These OF algorithms are then compared with the proposed algorithm. The large deformation diffeomorphism strategy [3, 4, 26, 23] and the metamorphoses strategy [24, 25] are also discussed in section 2. The new nudging strategy and its associated data assimilation strategy are presented in section 3. Differences between the proposed data assimilation strategy and some existing methods [20, 2] are also discussed. Using the thermal shallow water dynamical framework, numerical results are serving to support the proposed developments. Conclusion is given in Section 4. The complete code to reproduce the numerical results in this paper is available at 10.5281/zenodo.10252176.

2 A differential geometry formulation of the optimisation problem

Let (Ω, g) be a compact oriented Riemannian manifold of dimension n with or without boundary, in which g is the Riemannian metric. For any smooth vector field u, θ_u is the differential 1-form such that $\theta_u(v) = g(u, v) = \langle u, v\rangle$ for any smooth vector field v. Let $T\Omega$ be the tangent bundle of Ω and $T^*\Omega$ the cotangent bundle. For any smooth map $\phi : \Omega \longrightarrow \Omega$, ϕ_* refers to the push-forward map of $T\Omega$ induced by ϕ, and ϕ^* to the pull-back map of $T^*\Omega$ induced by ϕ. We further assume that ϕ is invertible, and

$$\phi^{\#} : T\Omega \cup T^*\Omega \longrightarrow T\Omega \cup T^*\Omega \tag{4}$$
$$u \longrightarrow \phi_* u \tag{5}$$
$$\omega \longrightarrow (\phi^{-1})^*\omega, \tag{6}$$

for any $u \in T\Omega$ and $\omega \in T^*\Omega$. It further induces an isomorphism of tensor fields of any specific type:

$$\phi^{\#} : V_1 \otimes V_2 \otimes \cdots \otimes V_l \longrightarrow V_1 \otimes V_2 \otimes \cdots \otimes V_l \tag{7}$$
$$\alpha_1 \otimes \alpha_2 \otimes \cdots \otimes \alpha_l \longrightarrow (\phi^{\#}\alpha_1) \otimes \cdots \otimes (\phi^{\#}\alpha_l) \tag{8}$$

in which V_i can either be a copy of $T\Omega$ or a copy of $T^*\Omega$.

For the smooth vector field u such that $u\big|_{\partial\Omega} \in i_*(T\partial\Omega)$, where $i : \partial\Omega \longrightarrow \Omega$ is the natural embedding map of the boundary, $\Phi_u : [0, \epsilon] \times \Omega \longrightarrow \Omega$ denotes the flow that satisfies

$$\frac{\partial \Phi_u(s, x)}{\partial s} = u(\Phi_u(s, x)). \tag{9}$$

The Lie derivative of any tensor field θ with respect to u is:

$$\mathcal{L}_u\theta = \lim_{s\to 0} \frac{\Phi_u(s)^{\#}\theta - \theta}{s}, \tag{10}$$

which is also a tensor field, of the same type as θ. To first order, a Taylor expansion gives:

$$\Phi_u(s)^{\#}\theta = \theta + s\mathcal{L}_u\theta + o(s). \tag{11}$$

The Riemannian metric g provides the inner product for the tangent space $T_x\Omega$ for any $x \in \Omega$. This inner product could be generalized to the space of tensor fields of any specific type. For $\theta_1, \theta_2 \in V_1 \otimes \cdots \otimes V_k$, the inner product induced by g at $x \in \Omega$ is written as $\langle\theta_1, \theta_2\rangle_x$. The corresponding norm writes $|\theta_2|_x^2 = \langle\theta_2, \theta_2\rangle_x$. The Riemannian metric further induces several operators. Let $*$ be the Hodge star operator, d the exterior derivative, and $\delta = (-1)^{n(k-1)+1} * d*$ the codifferential. These operators act on differential forms. The Laplacian operator is defined as $\Delta = d\delta + \delta d$. Let dV be the volume form on Ω.

Recall that θ_u is a differential 1-form determined by vector field u and the Riemannian metric tensor g. With the above notations, we can generalize the OF method for tensor fields on a Riemannian manifold:

Definition 2.0.1. *Let θ_1 and θ_2 be two tensor fields on Ω of the same type. When Ω is a compact oriented Riemannian manifold without boundary, solve for*

$$u = \underset{u\in T\Omega}{\arg\min} \int_\Omega \left[\frac{\partial|\theta_1 - \Phi_u(s)^{\#}\theta_2|_x^2}{\partial s}\Big|_{s=0} + a_1|d\theta_u|_x^2 + a_1|\delta\theta_u|_x^2 + a_0|\theta_u|_x^2 \right] dV. \tag{12}$$

When Ω is a compact oriented Riemannian manifold with boundary, solve for

$$\begin{cases} u = \underset{u\in T\Omega}{\arg\min} \displaystyle\int_\Omega \left[\frac{\partial|\theta_1 - \Phi_u(s)^{\#}\theta_2|_x^2}{\partial s}\Big|_{s=0} + a_1|d\theta_u|_x^2 + a_1|\delta\theta_u|_x^2 \right] dV \\ u\big|_{\partial\Omega} = i_*v, \end{cases} \tag{13}$$

where $v \in T\partial\Omega$ is the given boundary condition and i is the natural embedding of $\partial\Omega$.

Using the Taylor expansion of $\Phi_u^{\#}\theta_2$, see Eq.(11), Eq.(12) is equivalent to

$$u = \underset{u\in T\Omega}{\arg\min} \int_\Omega \left[-2\langle\theta_1 - \theta_2, \mathcal{L}_u\theta_2\rangle_x + a_1|d\theta_u|_x^2 + a_1|\delta\theta_u|_x^2 + a_0|\theta_u|_x^2 \right] dV, \tag{14}$$

and Eq.(13) equivalent to

$$\begin{cases} u = \underset{u\in T\Omega}{\arg\min} \displaystyle\int_\Omega \left[-2\langle\theta_1 - \theta_2, \mathcal{L}_u\theta_2\rangle_x + a_1|d\theta_u|_x^2 + a_1|\delta\theta_u|_x^2 \right] dV \\ u\big|_{\partial\Omega} = i_*v. \end{cases} \tag{15}$$

Theorem 2.1. *For θ_1, θ_2, and v with finite H^1 norm, i.e. $\int_\Omega |\theta_i|_x^2 + |d\theta_i|_x^2 + |\delta\theta_i|_x^2 < \infty$ for $i = 1, 2$, and similar for v, the optimisation problems* (14) *and* (15) *are always uniquely solvable in the space $H^1(T\Omega)$. And the solution is twice differentiable.*

Theorem 2.1 is a direct consequence of some proven mathematical results in [9] (or [22]). A complete demonstration is provided in the appendix. The formulation of (12) and (13), together with theorem (2.1) provide an option for the theory of defining and computing the displacement flow of two tensor fields. Due to Poincare lemma, both the regularization terms in (12) and (13) are equivalent to the H^1 norm. Still, the regularization term does not have to be the H^1 norm. For instance, $|d\delta\theta_u|_x^2 + |\delta d\theta_u|_x^2$ is considered in [5]. However, the vector field u calculated from Eq.(12) or (13) should not necessarily be the same as the true velocity field, largely depending on the regularization terms. True physical laws may not always be well represented by such regularization terms.

2.1 A detailed formulation of $T^{\#}$ for physical fields

We can now write down a more explicit expression for (2). Given two physical fields $S_1(x)$ and $S_2(x)$ that represent the same quantity S, we first associate a tensor to this state variable S. Thus S_1 and S_2 corresponds to two tensor fields, θ_1 and θ_2, of the same type. The displacement vector field u is then calculated based on (12) or (13) for θ_1 and θ_2. It is required that the correspondence between S and the tensor is 1-1 and onto, i.e. an unique S can be inferred from a given value of the tensor. Thus, for a given displacement map $T : \Omega \longrightarrow \Omega$, $T^{\#}S_2$ is defined in three steps:

1), construct tensor field θ_2 based on S_2;

2), $\theta_2^{\text{new}} \leftarrow T^{\#}\theta_2$;

3), $T^{\#}S_2$ is then inferred from θ_2^{new}.

Under $T^{\#}$, certain physical quantities will naturally be conserved as long as T is an diffeomorphism of Ω which preserves the orientation. Iteratively solving (2), a displacement flow $\Phi(s, x)$ can then be constructed. $\Phi(0, x) = x$, $\Phi(t_N)$ will also be a diffeomorphism that preserves the orientation. We demonstrate the conservative nature of $T^{\#}$ using the following examples.

Example 2.1.1. Suppose S denotes the density of a flow. We can associate S to a differential $n-$form: $\theta_S = SdV$, where dV is the volume form on Ω. Then for any 1-1 and onto map T that preserves the orientation of Ω,

$$(T^{\#}\theta_S)(x) = ((T^{-1})^*\theta_S)(x) = S(T^{-1}(x))(T^{-1})^*(dV) = S(T^{-1}(x))\alpha(x)dV, \tag{16}$$

in which α is some positive function. Thus $(T^{\#}S)(x) = S(T^{-1}(x))\alpha(x)$. We also have:

$$\int_\Omega SdV = \int_\Omega (T^{-1})^*(SdV) = \int_\Omega T^{\#}SdV. \tag{17}$$

This means that the total mass is conserved.

Example 2.1.2. Suppose that $S = u = (u^1, u^2)$ is the velocity field on a 2 dimensional domain in $\mathbb{R}^2$. We associate to S a differential $1-$form $\theta_S = u^1dx^1 + u^2dx^2$. Then for any 1-1 and onto map T which preserves the orientation of Ω, we have

$$\begin{aligned}&(T^{\#}\theta_S)(x) = ((T^{-1})^*\theta_S)(x)\\ =&\Big[u^1(T^{-1}(x))\frac{\partial(T^{-1})^1}{\partial x^1} + u^2(T^{-1}(x))\frac{\partial(T^{-1})^2}{\partial x^1}\Big]dx^1 + \Big[u^1(T^{-1}(x))\frac{\partial(T^{-1})^1}{\partial x^2} + u^2(T^{-1}(x))\frac{\partial(T^{-1})^2}{\partial x^2}\Big]dx^2\end{aligned} \tag{18}$$

This shows that

$$T^{\#}(u^1, u^2) = \Big(u^1(T^{-1}(x))\frac{\partial(T^{-1})^1}{\partial x^1} + u^2(T^{-1}(x))\frac{\partial(T^{-1})^2}{\partial x^1}, u^1(T^{-1}(x))\frac{\partial(T^{-1})^1}{\partial x^2} + u^2(T^{-1}(x))\frac{\partial(T^{-1})^2}{\partial x^2}\Big) \tag{19}$$

Since $d(T^{-1})^* = (T^{-1})^*d$, we have

$$\int_\Omega d\theta_S = \int_\Omega (T^{-1})^*(d\theta_S) = \int_\Omega d((T^{-1})^*\theta_S) = \int_\Omega d(T^{\#}\theta_S) \tag{20}$$

Note that $d\theta_S = (\frac{\partial u^2}{\partial x^1} - \frac{\partial u^1}{\partial x^2})dx^1 \wedge dx^2$. Therefore

$$\int_\Omega (\frac{\partial u^2}{\partial x^1} - \frac{\partial u^1}{\partial x^2})dx^1 \wedge dx^2 = \int_\Omega (\frac{\partial[T^{\#}(u^1, u^2)]^2}{\partial x^1} - \frac{\partial[T^{\#}(u^1, u^2)]^1}{\partial x^2})dx^1 \wedge dx^2, \tag{21}$$

in which $[T^{\#}(u^1, u^2)]^i$ denotes the $i-$th component of $[T^{\#}(u^1, u^2)]$. Hence the total vorticity is conserved.

2.2 A physical interpretation of the tensor field definitions

Described above for 2.1.1 and 2.1.2, the conservative nature of $T^{\#}$ largely depends on the choice of tensor fields. The question now translates on how to choose the adequate tensor fields. Since Eq.(11) describes how the tensor field changes along the vector field u, the Lie derivative in (11) shall closely relate to the transport equation of physical fields.

Example 2.2.1. Consider $\Omega \subset \mathbb{R}^2$ is a two dimensional domain, and the original dynamical equation for S

$$\frac{dS}{dt} := S_t + v \cdot \nabla S = 0, \tag{22}$$

in which $v(t, x)$ is the true velocity field in the system. Define the flow $\Phi(t, x)$:

$$\begin{cases} \frac{\partial \Phi}{\partial t}(t, x) = v(t, \Phi(t, x)) \\ \Phi(0, x) = x \end{cases} \tag{23}$$

Then Eq.(22) means that $S(t, \Phi(t, x)) = S(0, x)$ for any $t > 0$, i.e. S is conserved along the trajectory of each point. In this case, $\Phi(t) : \Omega \longrightarrow \Omega$ plays the role of a "true" displacement map. Recall that the goal is to find a displacement map T for given snapshots S_1 and S_2. Choose the tensor $\theta_S = S$, which is simply a function (or differential 0-form as a tensor field), the relation $S(t, \Phi(t, x)) = S(0, x)$ writes $\theta_S(t) = \Phi(t)^{\#}\theta_S(0)$. Correspondingly, we have $\mathcal{L}_u \theta_2 = u \cdot \nabla S_2$.

If the original dynamical equation for the physical field S is modified

$$\frac{dS}{dt} := S_t + v \cdot \nabla S = \text{(forcing terms)} \tag{24}$$

$S(0, x) \neq S(t, \Phi(t, x))$. However, we can still choose $\theta_S = S$. The minimization problem (2) shall search for the vector field u transporting S_2 towards S_1 the fastest along the virtual flow Φ_u. It is also equivalent to look for a virtual vector field u so that if S_2 is transported along u by the virtual system

$$\begin{cases} \frac{\partial \tilde{S}}{\partial s} + u \cdot \nabla \tilde{S} = 0 \\ \tilde{S}(0, x) = S_2 \end{cases} \tag{25}$$

in a virtual time interval $[0, \epsilon]$, then S_2 transforms the most rapidly towards S_1.

Example 2.2.2. Now, consider $\Omega \subset \mathbb{R}^n$ an $n-$dimensional domain with the original dynamical equation

$$S_t + \nabla \cdot (Sv) = 0, \tag{26}$$

with $v(t, x)$ the true velocity field. Similar to the previous example, define the flow $\Phi(t, x)$:

$$\begin{cases} \frac{\partial \Phi}{\partial t}(t, x) = v(t, \Phi(t, x)) \\ \Phi(0, x) = x \end{cases} \tag{27}$$

and the differential $n-$form $\theta(t, x) = S(t, x)dx^1 \wedge dx^2 \wedge \cdots \wedge dx^n$. Distinct from example 2.2.1, Eq.(26) implies that $\Phi(t)^*\theta(t, x) = \theta(0, x)$, or equivalently, $\theta(t, x) = (\Phi(t)^{-1})^*\theta(0, x) = \Phi(t)^{\#}\theta(0, x)$. Indeed, direct calculation yields:

$$\begin{aligned}
&\Phi(t + \Delta t)^*\theta(t + \Delta t, x) - \Phi(t)^*\theta(t, x) && (28)\\
=&\Phi(t)^*\Phi^*_{t\to t+\Delta t}\theta(t + \Delta t) - \Phi(t)^*\theta(t) && (29)\\
=&\Phi(t)^*\Big[(\Phi^*_{t\to t+\Delta t} - Id)\theta(t + \Delta t) + \theta(t + \Delta t) - \theta(t)\Big] && (30)\\
=&\Phi(t)^*\Big[(\Phi^*_{t\to t+\Delta t} - Id)\theta(t) + \theta(t + \Delta t) - \theta(t)\Big] + o(\Delta t) && (31)\\
=&\Delta t\Phi(t)^*\Big[\mathcal{L}_{v(t)}\theta(t) + \theta_t(t)\Big] + o(\Delta t) && (32)\\
=&\Delta t\Phi(t)^*\Big[\Big(S_t(t, x) + \nabla \cdot (S(t, x)v(t))\Big)dx^1 \wedge \cdots \wedge dx^n\Big] + o(\Delta t) && (33)\\
=&o(\Delta t) && (34)
\end{aligned}$$

It shows that $\Phi(t)^*\theta(t, x)$ does not change with time.

In both examples, the choice of tensor θ is determined by the original transport equation (22) or (26). This choice then implies $T^{\#}$, and the minimization problem (2) will search for a vector field u that most rapidly transports S_2 towards S_1 by a virtual flow Φ_u. For geophysical fields, $T^{\#}$ is thus essential for the application of this method, and further discussed in section 3.

2.3 Comparison with OF algorithms

Given a time series of snapshots (i.e. brightness fields in $\Omega \subset \mathbb{R}^2$) $\{..., S(t-\Delta t), S(t), S(t+\Delta t), ...\}$, the [1] OF algorithm aims at recovering the true velocity field $u(t,x)$ by minimizing the following functional (with proper boundary conditions):

$$u(t) = \arg\min_u \|S_t + \langle \nabla S, u\rangle\|^2 + a_1\|\nabla u\|^2 = \arg\min_u \int_\Omega [S_t + \langle \nabla S, u\rangle]^2 + a_1|\nabla u|^2 d^n x. \tag{35}$$

We remark that the first term implies that the hidden $T^\#$ in (35) is simply $T^\# S = S\circ T^{-1}$ for the brightness field S. Or equivalently, $T^\# S$ is inferred from $T^\#\theta_S$, where $\theta_S = S$ is a differential $0-$form. Indeed, for any vector field u, let $\Phi_u(s,x) : [0,\Delta t]\times\Omega \longrightarrow \Omega$ be the following flow of the points in the domain:

$$\begin{cases} \frac{\partial \Phi_u(s,x)}{\partial s} = u(\Phi_u(s,x)) \\ \Phi_u(0,x) = x. \end{cases} \tag{36}$$

The first term in (35) represents the material derivative of $S(t+s, \Phi_u(s,x))$ with respect to s at $s=0$. The optimisation problem (35) searches for vector field $\mathbf{u}$ so that $S(t,x) \approx S(t+\Delta t, \Phi_u(\Delta t, x))$. Let $S_2(x) = S(t,x)$, $S_1(x) = S(t+\Delta t, x)$, and $T(x) = \Phi_u(\Delta t, x)$. Hence the first term in (35) searches for the vector field u so that $S_1(x) \approx S_2(T^{-1}(x))$. Clearly, this implies that $T^\# S_2 = S_2\circ T^{-1}$. [16] generalizes this original OF method to the Riemannian manifold context. Still, the formulation of the problem in [16] implies that $T^\# S_2 = S_2 \circ T^{-1}$.

In [29], an other variant is proposed, to minimize

$$u(t) = \arg\min_u \|S_t + \nabla\cdot(Su)\|^2 + a_1\|\nabla u\|^2 = \arg\min_u \int_\Omega [S_t + \nabla\cdot(Su)]^2 + a_1|\nabla u|^2 d^n x. \tag{37}$$

Let $S_1(x) = S(t+\Delta t, x)$ and $S_2(x) = S(t,x)$. Following the analysis in example 2.2.2, Eq.(37) aims at finding the vector field u so that $\Phi_u^\# S_2 \approx S_1$, in which $\Phi_u^\# S$ is inferred from $\Phi_u^\#\theta_S$ for $\theta_S = S dx^1\wedge\cdots\wedge dx^n$. Thus, it can be concluded that the method of [29] implies that $T^\#$ should be defined as if the physical fields are associated to differential $n-$forms. This is explicitly stated in [28] and corresponds to physically-constrained choices of tensor fields in the present framework. The proper choices of tensor fields shall indeed enable to also transport unobserved state variables, consistent with the underlying dynamics. OF algorithms can thus be reformulated for snapshots corresponding to snapshots of tensor fields. For a time series $\{\cdots, \theta(t-\Delta t), \theta(t), \theta(t+\Delta t), \cdots\}$ of snapshots of tensor fields, the generalized OF method is to find the vector field u:

$$u(t) = \arg\min_u \int_\Omega |\theta_t + \mathcal{L}_u\theta|_x^2 + a_1|\nabla u|_x^2 dV, \tag{38}$$

in which u satisfies proper boundary conditions. Here we provide a theorem for the existence of the OF solution for Dirichlet boundary condition. Note that in [1], u is only required to have zero normal component at the boundary.

Theorem 2.2. *For fixed t, assume that both tensor fields θ and θ_t have finite H^2 norm and the given vector field v on $\partial\Omega$ also has finite H^1 norm. Further assume that $|d\theta|_x, |\delta\theta|_x$ are bounded in Ω. Then for compact oriented Riemannian manifold Ω without boundary, the following minimisation problem has a unique solution which has a finite H^1 norm:*

$$u(t) = \arg\min_{u\in H^1(T\Omega)} \int_\Omega |\theta_t + \mathcal{L}_u\theta|_x^2 + a_0|\theta_u|_x^2 + a_1|d\theta_u|_x^2 + a_1|\delta\theta_u|_x^2 dV. \tag{39}$$

For a compact oriented Riemannian manifold with boundary, the following minimisation problem has a unique solution which has a finite H^1 norm:

$$\begin{cases} u(t) = \arg\min_{u\in H^1(T\Omega)} \int_\Omega |\theta_t + \mathcal{L}_u\theta|_x^2 + a_1|d\theta_u|_x^2 + a_1|\delta\theta_u|_x^2 dV \\ u(t)\big|_{\partial\Omega} = v. \end{cases} \tag{40}$$

The existence, uniqueness, and smoothness of order 1 of the solution is a direct consequence of Riesz representation (or Lax-Milgram) theorem. A mathematical proof is provided in the appendix.

While the proposed algorithm can be applied whenever two snapshots are provided, the OF algorithms require that the time between two consecutive images to be small, to best approximate θ_t. To overcome such a constrain, the standard Horn and Schunck algorithm can be incorporated within a multi-scale strategy [18], and wavelets [8]. Note, an infinitesimal formulation of the Horn and Schunck algorithm in the Euclidean space is proposed in [8].

2.4 Comparison with other methods

[25] proposes a variational method to find the optimal way to transport a point $S_2 \in \mathcal{M}$ to another point $S_1 \in \mathcal{M}$ at a minimal cost. Here $\mathcal{M}$ is a Riemannian manifold. For geophysical applications, this manifold $\mathcal{M}$ can be interpreted as the configuration space. Hence each point $S_i \in \mathcal{M}$ represents a state vector. It can be interpreted in a way that, to transport S_2 to S_1, [25] does not only use vector fields, but also an external forcing to influence the state at each time step. The solution of the variational problem then consists of a time sequence of vector fields and a time sequence of "external forcing". Considering an "external forcing", the eventual state $T^{\#}S_2$ can exactly match the target state S_1. This method follows from rigorous mathematical developments [24], but turns out to be very computationally demanding.

Some efforts about large deformation diffeomorphic metric matching (LDDMM) [3, 4] are examples of directly solving (1) to obtain a diffeomorphism T belonging to the same connected component as the identity map in the group of diffeomorphisms $\mathcal{D}(\Omega)$. Since an external forcing is not considered, these methods can be stated to be simplified versions of that proposed by [25]. The regularization term in (1) is chosen to be

$$\|T\|^2 = \int_0^1 \|v(t)\|_V^2 dt \tag{41}$$

for some prescribed norm V. And $T(x) \approx (Id + 1/Nv_{\frac{N-1}{N}}) \circ \cdots \circ (Id + 1/Nv_0)$ as described in the introduction. Note that the optimisation problem in [3, 4] is a specific case of Eq.(6) in [26] and Eq.(1) in [23]. Despite the fact that $T^{\#}$ in [3, 4, 26, 23, 25] is not particularly designed for geophysical fields and sometimes the boundary condition is ignored, the framework proposed in this manuscript can be stated to be a simplified version of LDDMM.

2.5 About the boundary condition of (13)

Boundary condition is necessary in the optimisation problem (13). In fact, the boundary condition can be obtained by solving for (12) or (13) based on the data on $\partial\Omega$. The process can be illustrated using the following idealistic example.

Suppose that Ω is a three dimensional ocean, the boundary of which consists of two parts Ω_b and Ω_s, in which Ω_b refers to the ocean basin (i.e. the land boundaries), and Ω_s the sea surface. To determine the boundary condition of u on Ω_b and Ω_s, it is first natural to set $u\big|_{\Omega_b} = 0$. On Ω_s, we must first solve for (13) where θ_1 and θ_2 are tensor fields on Ω_s. Boundaries of Ω_s coincide with the coast lines, and natural to set boundary conditions to be 0. The domain Ω_s is a sub-manifold of the sphere. Hence the “Riemannian" context is necessary for this example. The complete process at each iterative step is illustrated in Algorithm 1.

Algorithm 1: How to determine the boundary condition at each iterative step (an example)

Data: tensor fields θ_1 and θ_2 on Ω; tensor fields α_1, α_2 on Ω_s; small positive number $\epsilon > 0$; the total number of iterations N; dV_s the volume form on Ω_s; dV the volume form on Ω.
Result: vector fields $u_1, ..., u_N$

for $i = 1, 2, ..., N$ **do**

$u_{s,i} \leftarrow \underset{u \in T\Omega_s}{\arg\min} \int_{\Omega_s} \Big[-2\langle \alpha_1 - \alpha_2, \mathcal{L}_u \alpha_2 \rangle_x + |d\theta_u|_x^2 + |\delta\theta_u|_x^2 \Big] dV_s$ with boundary condition $u_{s,i}\big|_{\partial\Omega_s} = 0$;

$u_i \leftarrow \underset{u \in T\Omega}{\arg\min} \int_{\Omega} \Big[-2\langle \theta_1 - \theta_2, \mathcal{L}_u \theta_2 \rangle_x + |d\theta_u|_x^2 + |\delta\theta_u|_x^2 \Big] dV$ with boundary condition $u_i\big|_{\Omega_b} = 0$,

$u_i\big|_{\Omega_s} = u_{s,i}$;

$\theta_2 \leftarrow \theta_2 + \epsilon \mathcal{L}_{u_i} \theta_2$;

$\alpha_2 \leftarrow \alpha_2 + \epsilon \mathcal{L}_{u_{s,i}} \alpha_2$

end

2.6 The case for localized observations

In practice, it is a common situation that some state variables are solely observed in a subdomain $\Omega_1 \subset \Omega$, instead of in the full domain Ω (i.e. over a satellite swath). A weight function W can be constructed and the first terms in Eq.(12) and (13) replaced by:

$$\frac{\partial |\theta_1 - \Phi_u(s)^{\#}\theta_2|_x^2}{\partial s}\Big|_{s=0} W(x), \tag{42}$$

in which the pre-chosen $W(x)$ takes value 1 for a majority of points inside Ω_1 but decreases to 0 smoothly as x approaches the boundary of Ω_1. Then Eq.(14) changes to

$$u = \underset{u\in T\Omega}{\arg\min} \int_\Omega \left[-2\langle\theta_1 - \theta_2, \mathcal{L}_u\theta_2\rangle_x W(x) + a_1|d\theta_u|_x^2 + a_1|\delta\theta_u|_x^2 + a_0|\theta_u|_x^2 \right] dV, \tag{43}$$

and Eq.(15) changes to

$$\begin{cases} u = \underset{u\in T\Omega}{\arg\min} \int_\Omega \left[-2\langle\theta_1 - \theta_2, \mathcal{L}_u\theta_2\rangle_x W(x) + a_1|d\theta_u|_x^2 + a_1|\delta\theta_u|_x^2 \right] dV \\ u\big|_{\partial\Omega} = i_* v. \end{cases} \tag{44}$$

The theorem of existence and uniqueness of solution still holds for minimisation problems (43) and (44) following similar arguments given in the appendix.

3 Towards a new nudging strategy and its application in data assimilation

3.1 Methodology

Let S be the full state variable, $Y = h(S)$ some state variable derived from S. Assume that we have the model estimate S_{model}, and that Y is fully observed on the domain. Our target is to

(1), derive a displacement flow Φ so that $\Phi^\# Y^{\text{model}} \approx Y^{\text{obs}}$;

(2), apply Φ to S^{model} to correct the displacement of the full state variable S.

From section 2, we need to separately find the tensor fields for Y and S. Consistent definitions should be determined by the dynamical equation of the system, leading to the determination of $T^\#$, hence the explicit formulation of Eq.(14) (or (15)).

Already indicated in [2] and [20], this nudging strategy can be incorporated with ensemble Kalman filter. The basic idea is to correct the displacement of each ensemble member before applying EnKF. Methods reported in [2] and [20] use different cost functions to estimate the displacements. Both methods implicitly assume $T^\# S = S\circ T$ or $S\circ T^{-1}$. However, see Fig.2, $T^\#$ without considering the dynamics could possibly destroy the intrinsic feature of the unobserved physical fields.

To demonstrate the advantage to consistently constrain $T^\#$, the following simple version of morphed EnKF is compared numerically with the plain EnKF algorithm:

(1), choose tensor fields for the observed state variable Y and the full state variable X;

(2), find the displacement flow Φ_i according to the observation Y^{obs} and the model estimates Y_i^{model} from the $i-$th ensemble member;

(3), apply Φ_i to the full state vector of the $i-$th ensemble member: $X_i^f \leftarrow \Phi_i^\# X_i^f$;

(4), apply plain EnKF to the updated ensemble $\{X_i^f\ i = 1, ..., N_e\}$.

A morphed ensemble member based on the plain $T^\# S = S\circ T^{-1}$ is also presented for comparison.

3.2 Numerical results

To illustrate our purpose, a data assimilation experiment is conducted for only one time step, using the thermal shallow water equation [27]. This model consists of three state variables: $h-$the water height, $v = (v^1, v^2)-$the velocity field, and $\Theta-$the buoyancy (or density contrast):

$$\frac{\partial h}{\partial t} + \nabla\cdot(hv) = 0, \tag{45}$$

$$\frac{\partial\Theta}{\partial t} + (v\cdot\nabla)\Theta = -\kappa(h\Theta - h_0\Theta_0), \tag{46}$$

$$\frac{\partial v}{\partial t} + (v\cdot\nabla)v + f\hat{z}\times v = -\nabla(h\Theta) + \frac{1}{2}h\nabla\Theta. \tag{47}$$

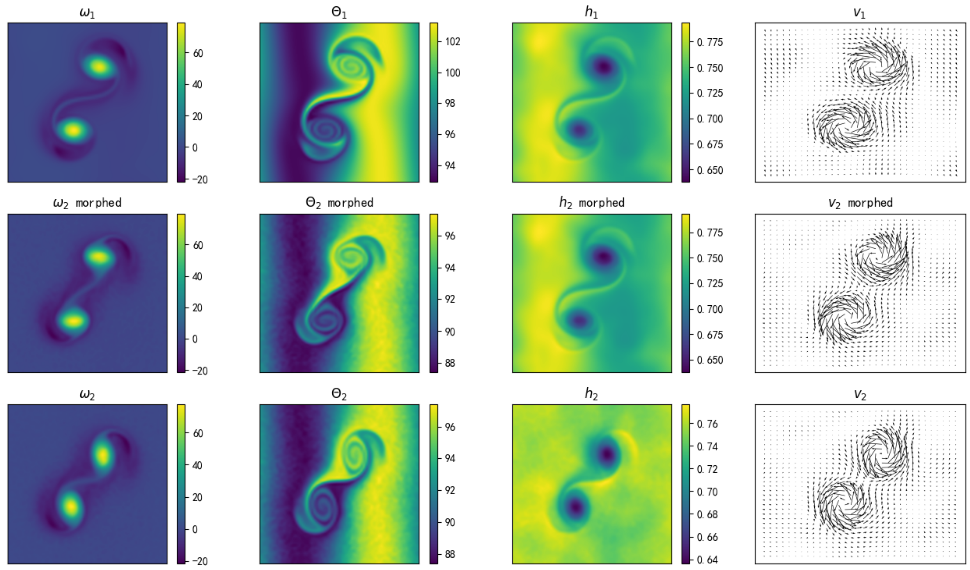

Figure 3: Comparison of the target fields (the first row), the original fields (the third row), and the morphed fields (the second row).

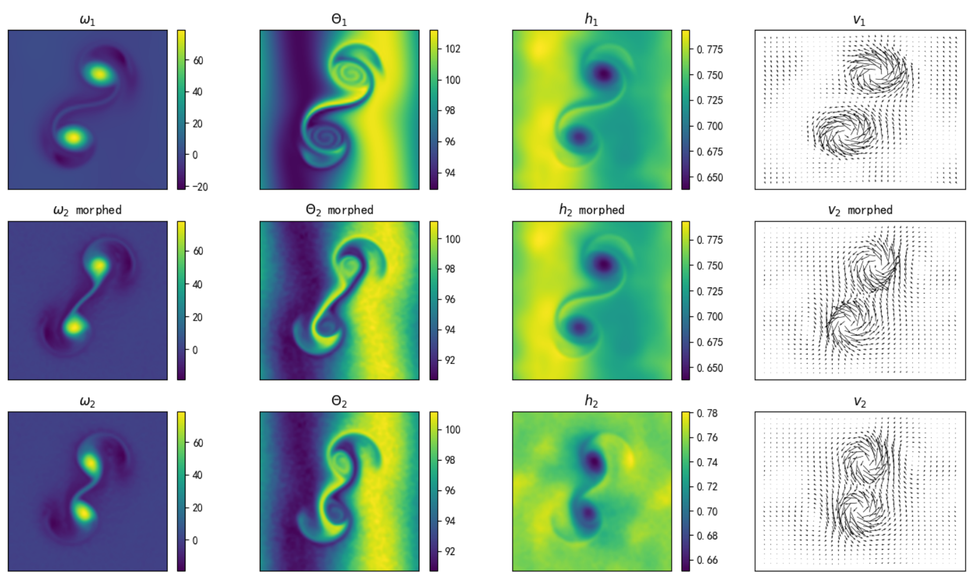

Figure 4: Another example of Fig.3

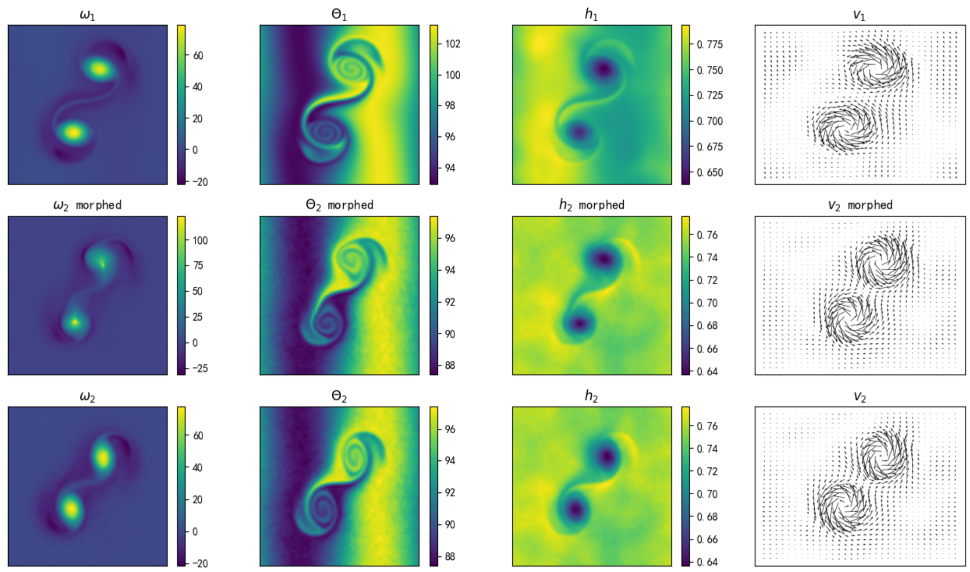

Figure 5: The target field (first row), the original field (third row), and the field morphed by $T^{\#}S = S \circ T^{-1}$ for $S = h, \omega, \Theta, v^1, v^2$ (second row).

Both Θ and h are assumed strictly positive at each point. It is assumed that both the absolute vorticity $\omega = \frac{\partial v^2}{\partial x} - \frac{\partial v^1}{\partial y}$ and h are fully observed, while Θ is completely unobserved. The details of the experimental setup can be found in the appendix. A Python code to completely reproduce the numerical results is provided at 10.5281/zenodo.10252176.

Fig.3 and Fig.4 show two examples of the (interpolated) truth (the target fields), the prior estimate of one member (the original fields), and the morphed prior estimate (the morphed fields). Expected, the phase of the original vortex can be adjusted, to some extent, but not perfectly. This is not surprising because the cost function in the optimisation problem (12) (or (13)) has two parts. The first part is derived from the dynamics of the original system. But the second part is merely for mathematical reasons. Thus, the virtual displacement flow Φ cannot transform Θ_2 to exactly match Θ_1. But the correct choice of tensor fields can maintain the dynamical balance of the three fields during the morphing process to some extent. Looking at Fig.3 and 4 more closely, it is found that the difference between the morphed h_2 field and the target h_1 field is much smaller than that between the morphed ω_2 and the target ω_1. We don't have a theoretical explanation of this fact. We suspect that it can be attributed to the positiveness of the h field.

To demonstrate the superiority of $T^{\#}$, the nudging process without introducing the concept of tensor fields is also considered and tested. In this case, $T^{\#}S = S \circ T^{-1}$, independent of $S = h$, ω, Θ, or v^1, v^2. The initial value of ω_2 h_2, etc. are taken to be the corresponding fields of one of the ensemble priors. We first run the morphing process for $N = 10000$ time steps. It is found that, for this specific member, the mean-squared-error (MSE) of h is always decreasing, while the MSE for ω decreases till $N \approx 6000$ and then starts to increase. The fields at $N = 6000$ are plotted in Fig.5. Apparently, the morphed ω_2 has lost its intrinsic feature.

Fig. 6 presents the truth, the prior mean of the ensemble, and the prior mean of the morphed ensemble. The direct prior mean has completely lost the small scale structures inside the vortex, while the prior mean of the morphed ensemble still maintain the small scale features to some extent. Stated in the introduction, our interpretation is that $y^o - x^b$ is no longer a good representation of the error in this case. Instead, the location error, or more generally the displacement flow, can better represent the error of each ensemble member. Thus the space of ensemble members is not a linear subspace in the Euclidean space of the state vector, but could be a curved manifold. In this case, it is not surprising to see that the arithmetic mean lies outside of the manifold. To address this problem, the Fréchet mean instead of the arithmetic mean should be used to define the ensemble mean.

Fig.7 presents the posterior estimate of one ensemble member using EnKF and morphed EnKF (denoted by mEnKF for short). Apparently, the plain EnKF results in erroneous estimates, while the mEnKF still produces reasonable

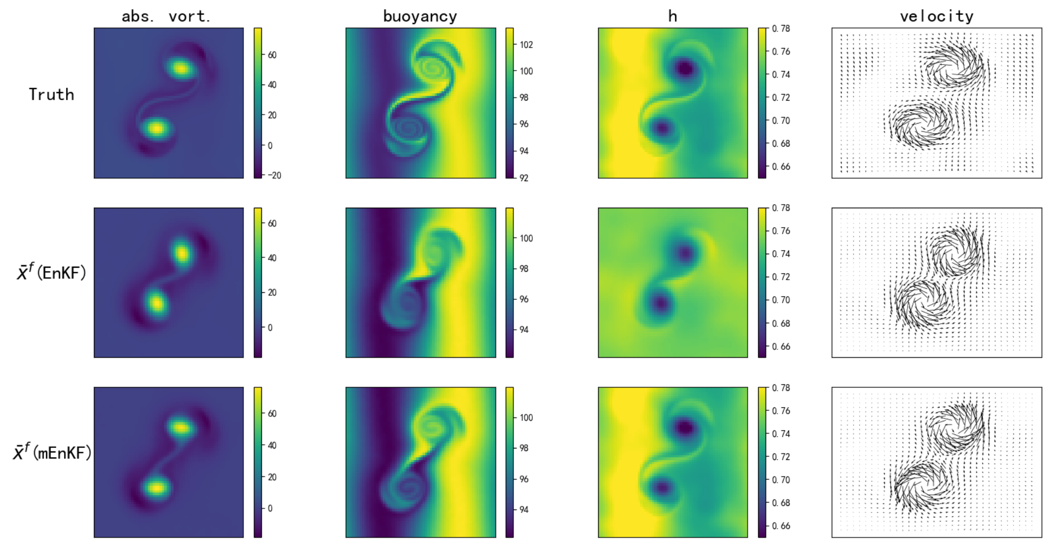

Figure 6: The truth (first row), the prior mean of ensemble (the second row), and the prior mean of the morphed ensemble (the third row).

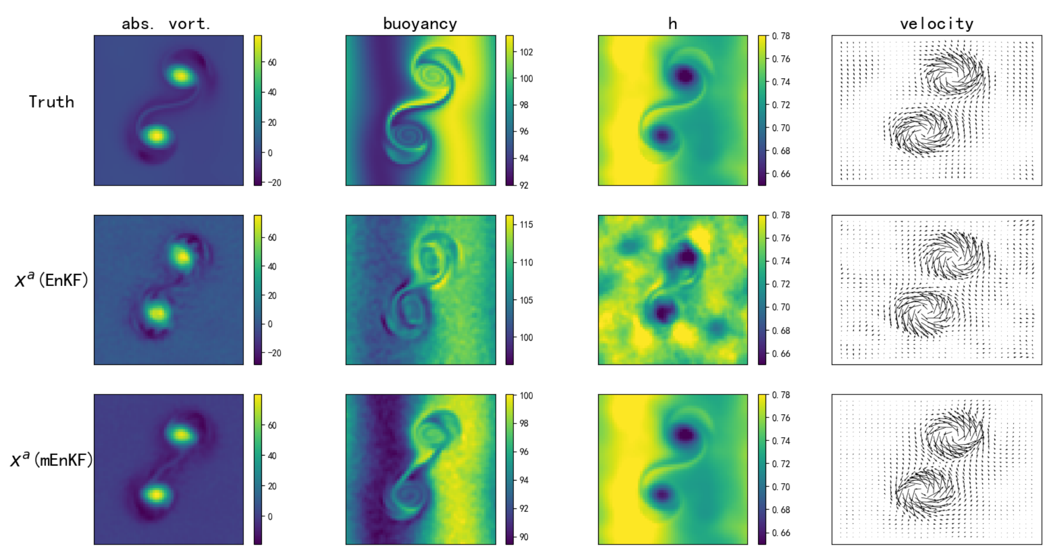

Figure 7: The truth (first row), the posterior estimate of one member (the second row), and the posterior estimate of one morphed member (the third row).

estimates with fine scale features inside the vortex. Again, this is the disadvantage of linear algorithms when the ensemble members do not lie on a linear subspace of the Euclidean space of state vectors.

4 Conclusion

A complete framework is introduced to estimate the displacement flow between two tensor fields on a compact oriented Riemannian manifold with or without boundary. It is proved that the solution always exists and is unique. When a time sequence of snapshots of geophysical fluids is available, a reformulation of the generalized OF algorithm [28] can also be obtained from this differential geometry perspective.

The novelty of the proposed framework lies in the definition of $T^{\#}S$ for a given displacement map T (not necessarily the displacement generated by the true velocity field) acting on a given state variable S: $T^{\#}S$ must be determined by the original dynamics of S. Technically, each state variable S is associated to a tensor field θ_S, and $T^{\#}S$ is determined by $T^{\#}\theta_S$. A key advantage is to consistently correct the displacement of some state variable while best maintaining the intrinsic structure of the underline physical fields.

This new framework can then be used as a nudging process when only part of the state variables are observed. It can also be used to correct the displacement of each ensemble member before applying the linear EnKF algorithm. Numerical results with a double-vortex model show that the morphed EnKF algorithm produces more reliable posterior estimates than the plain EnKF algorithm. The preferable usage of $T^{\#}$ is well demonstrated by comparing fields morphed by algorithms derived or not from the concepts of differential geometry.

It must be pointed out that all physical fields could not always be associated to a tensor field. The use of a tensor field is only required to define the correct $T^{\#}$. For an arbitrary derived physical field S, $T^{\#}S$ should be determined by the forward operator $S = F(X)$, where X is the full state vector. Thus, for a specific derived variable S, whether a displacement vector field can be determined by the optimisation procedure (12) or (13) needs to be further studied.

Acknowledgments

The authors would like to express their gratitude to Long Li at the department of mathematics of ShanghaiTech University and Wei Pan at department of mathematics of Imperial College London for their insightful and helpful discussion, and and Etienne Mémin for his introduction on relevant works. YZ's research is supported by Hohai university (Grant No. 1074-423101 and 522-020512). VR's research is supported by the company SCALIAN DS and by France Relance through the MORAANE project. BC's research is supported by ERC EU SYNERGY Project No. 856408-STUOD, and the the support of the ANR Melody project.

Appendices

A Proof of theorem 2.1

Recall that d is the exterior derivative operator, $*$ the Hodge star operator on differential forms, and $\delta = (-1)^{n(k-1)+1} * d*$ is the so-called co-differential operator. Let $i : \partial\Omega \to \Omega$ be the natural embedding of $\partial\Omega$. For convenience but without loss of generality, we set the regularization parameter $a_0 = a_1 = 1$.

First, consider the case when Ω is a compact oriented Riemannian manifold with boundary. Assume that u is a solution of (15). Then for any vector field $h \in T\Omega$ such that $h\big|_{\partial\Omega} = 0$, we have

$$\frac{\partial}{\partial\epsilon}\Big[\int_\Omega -2\langle\theta_1 - \theta_2, \mathcal{L}_{u+\epsilon h}\theta_2\rangle_x + |d\theta_{u+\epsilon h}|_x^2 + |\delta\theta_{u+\epsilon h}|_x^2 dV\Big]\Big|_{\epsilon=0} = 0 \tag{48}$$

This implies that for any $h \in T\Omega$ such that $h\big|_{\partial\Omega} = 0$,

$$\int_\Omega -2\langle\theta_1 - \theta_2, \mathcal{L}_h\theta_2\rangle_x + \langle d\theta_u, d\theta_h\rangle_x + \langle\delta\theta_u, \delta\theta_h\rangle_x dV = 0 \tag{49}$$

Applying the Green's formula for differential forms (see for instance Eq.(2.1) in [9]), we have that

$$\int_\Omega \langle d\theta_h, d\theta_u\rangle_x dV - \int_\Omega \langle\theta_h, \delta d\theta_u\rangle_x dV = \int_{\partial\Omega} (i^*\theta_h) \wedge *(i^* d\theta_u) = 0 \tag{50}$$

since $\theta_h\big|_{\partial\Omega} = 0$. Similarly,

$$\int_\Omega \langle d\delta\theta_u, \theta_h\rangle_x dV - \int_\Omega \langle\delta\theta_u, \delta\theta_h\rangle_x dV = \int_{\partial\Omega} (i^*\delta\theta_u) \wedge *(i^*\theta_h) = 0. \tag{51}$$

Thus

$$\int_\Omega \langle d\theta_u, d\theta_h\rangle_x + \langle\delta\theta_u, \delta\theta_h\rangle dV = \int_\Omega \langle\theta_h, (d\delta + \delta d)\theta_u\rangle_x dV = \int_\Omega \langle\theta_h, \Delta\theta_u\rangle_x dV, \tag{52}$$

where $\Delta = d\delta + \delta d$ is the Hodge Laplacian operator.

Let $\alpha = \theta_1 - \theta_2, \beta = \theta_2$. By partition of unity, $\langle\alpha, \mathcal{L}_h\beta\rangle$ can be decomposed into a finite sum:

$$\langle\alpha, \mathcal{L}_h\beta\rangle = \sum_i \langle\alpha_i, \mathcal{L}_h\beta_i\rangle, \tag{53}$$

in which α_i's and β_i's have the same regularity as α and β, and are all of the form $\eta_1 \otimes \cdots \otimes \eta_l$, with $\eta_j \in V_j$ and $V_j = H^1(T\Omega)$ or $H^1(T^*\Omega)$. Note that

$$\mathcal{L}_h(\eta_1 \otimes \cdots \otimes \eta_l) = \mathcal{L}_h\eta_1 \otimes \eta_2 \otimes \cdots \otimes \eta_l + \cdots + \eta_1 \otimes \cdots \otimes \eta_{l-1} \otimes \mathcal{L}_h\eta_l, \tag{54}$$

Thus there exists, finitely, many known numbers m_i and known $\xi_i, \eta_i \in T\Omega$ or $\xi_i, \eta_i \in T^*\Omega$, so that

$$\langle\alpha, \mathcal{L}_h\beta\rangle = \sum_i m_i\langle\xi_i, \mathcal{L}_h\eta_i\rangle. \tag{55}$$

Since for any $\xi, \eta \in T\Omega$, $\langle\xi, \mathcal{L}_h\eta\rangle = -\langle\theta_\eta, \mathcal{L}_h\theta_\xi\rangle$, in which θ_ξ (or θ_η) refers to the differential 1-form such that $\theta_\xi(v) = \langle\xi, v\rangle$ (or $\theta_\eta(v) = \langle\eta, v\rangle$ resp.) for any vector field $v \in T\Omega$, without loss of generality we can assume that all the ξ_i's and η_i's in Eq. (55) are differential 1-forms. With Cartan's formula $\mathcal{L}_h = d\iota_h + \iota_h d$ and Stokes' formula, we have

$$\begin{aligned}
&\int_\Omega -2\langle\theta_1 - \theta_2, \mathcal{L}_h\theta_2\rangle_x dV = \int_\Omega -2\langle\alpha, \mathcal{L}_h\beta\rangle_x dV = -2\int_\Omega \sum_i m_i\langle\xi_i, \mathcal{L}_h\eta_i\rangle_x dV \\
=& -2\int_\Omega \sum_i m_i\mathcal{L}_h\eta_i \wedge *\xi_i = -2\sum_i \int_\Omega [(d\iota_h + \iota_h d)\eta_i] \wedge *(m_i\xi_i) \\
=& -2\sum_i \int_\Omega d[\iota_h\eta_i \wedge *(m_i\xi_i)] - \iota_h\eta_i \wedge d*(m_i\xi_i) + \iota_h d\eta_i \wedge *(m_i\xi_i) \\
=& -2\Big\{\sum_i \int_{\partial\Omega} \iota_h\eta_i \wedge *(m_i\xi_i) + \int_\Omega -\iota_h\eta_i \wedge d*(m_i\xi_i) + \iota_h d\eta_i \wedge *(m_i\xi_i)\Big\} \\
=&2\sum_i \int_\Omega \iota_h\eta_i \wedge d*(m_i\xi_i) + \iota_h d\eta_i \wedge *(m_i\xi_i)
\end{aligned} \tag{56}$$

For any differential 1-form θ, denote by $X_\theta \in T\Omega$ the vector field such that $\langle \eta, \theta \rangle = \eta(X_\theta)$ for any $\eta \in T^*\Omega$. Then

$$
\begin{aligned}
&\iota_h d\eta_i \wedge *(m_i\xi_i) = \langle \iota_h d\eta_i, m_i\xi_i \rangle_x dV \\
=&(\iota_h d\eta_i)(X_{m_i\xi_i})dV = d\eta_i(h, X_{m_i\xi_i})dV = -d\eta_i(X_{m_i\xi_i}, h)dV \\
=& -(\iota_{X_{m_i\xi_i}} d\eta_i)(h)dV = -\langle \iota_{X_{m_i\xi_i}} d\eta_i, \theta_h \rangle_x dV,
\end{aligned}
\tag{57}
$$

and

$$
\begin{aligned}
&\iota_h \eta_i \wedge d*(m_i\xi_i) = \langle \iota_h \eta_i, *d*m_i\xi_i \rangle_x dV = \langle \theta_h(X_{\eta_i}), *d*(m_i\xi_i) \rangle_x dV \\
=&\theta_h(X_{\eta_i}) * d*(m_i\xi_i)dV = \langle \theta_h, [*d*(m_i\xi_i)]\eta_i \rangle dV
\end{aligned}
\tag{58}
$$

It thus exists a differential 1-form $\mu \in L^2(T^*\Omega)$, which is determined by η_i, m_i, ξ_i, so that

$$
\int_\Omega 2\langle \theta_1 - \theta_2, \mathcal{L}_h\theta_2 \rangle_x dV = \int_\Omega \langle \theta_h, \mu \rangle_x dV. \tag{59}
$$

Combining Eq.(52) and (59), Eq.(49) is equivalent to

$$
\int_\Omega -\langle \theta_h, \mu \rangle_x + \langle \theta_h, \Delta\theta_u \rangle_x dV = 0. \tag{60}
$$

Thus the optimisation problem (13) is equivalent to solving the following equation for θ_u:

$$
\begin{cases}
\Delta\theta_u = \mu \\
\theta_u\big|_{\partial\Omega} = \theta_{\widetilde{i_* v}}\big|_{\partial\Omega},
\end{cases}
\tag{61}
$$

in which $\widetilde{i_* v}$ is a smooth extension of v from $\partial\Omega$ to Ω. Then the existence, uniqueness, and smoothness of the solution to (61) is then guaranteed by theorem (3.4.10) of [22].

For the case, Ω a compact and oriented Riemannian manifold without boundary, the optimisation problem (12) is equivalent to solving the following equation for differential 1-forms:

$$
(1 - \Delta)\theta_u = \mu, \tag{62}
$$

where μ is a differential 1-form that can be derived from the given data. The spectral theory of Laplacian operator on a Riemannian manifold (see for instance theorem (1.30) and (1.31) in [21]) states that the space of square integrable differential $k-$forms $W^{0,2}(\bigwedge^k T^*\Omega)$ has an orthonormal basis $\{\phi_i : \Delta\phi_i = \lambda_i\phi_i, \int_\Omega \langle \phi_i, \phi_i \rangle_x dV = 1, 0 \leq i < \infty\}$, and that all eigen-forms ϕ_i are smooth on Ω. Note that $\lambda_i \leq 0\ \forall i$. Thus we can assume the decomposition: $\mu = \sum_{i\geq 0} a_i\phi_i$. Then $\theta_u = \sum_i \frac{a_i}{1-\lambda_i}\phi_i$ is a solution to Eq.(62). The identity can be verified directly. But in addition we need to show that $\theta_u \in W^{2,2} = \{\theta : \int_\Omega \langle d\delta\theta, d\delta\theta \rangle_x + \langle \delta d\theta, \delta d\theta \rangle_x dV < \infty\}$. First we show that $\theta_u \in W^{1,2} = \{\theta : \int_\Omega \langle d\theta, d\theta \rangle_x + \langle \delta\theta, \delta\theta \rangle_x dV < \infty\}$. This can be verified directly:

$$
\begin{aligned}
&\int_\Omega \langle d\theta_u, d\theta_u \rangle_x + \langle \delta\theta_u, \delta\theta_u \rangle_x dV = \lim_{N\to\infty} \sum_{i=0}^N \frac{a_i^2}{1-\lambda_i} \int_\Omega \langle d\phi_i, d\phi_i \rangle_x + \langle \delta\phi_i, \delta\phi_i \rangle_x dV \\
=& \lim_{N\to\infty} \sum_i \frac{a_i^2}{1-\lambda_i} \int_\Omega \langle \delta d\phi_i, \phi_i \rangle_x + \langle d\delta\phi_i, \phi_i \rangle_x dV = \lim_{N\to\infty} \sum_i \frac{\lambda_i a_i^2}{1-\lambda_i} \leq \sum_i |a_i|^2
\end{aligned}
\tag{63}
$$

This shows that $\theta_u \in W^{1,2}$. Next, direct calculation yields that $\int_\Omega \langle \Delta\theta, \Delta\theta \rangle_x dV = \int_\Omega \langle d\delta\theta, d\delta\theta \rangle_x + \langle \delta d\theta, \delta d\theta \rangle_x dV$ for any θ. Hence

$$
\int_\Omega \langle d\delta\theta_u, d\delta\theta_u \rangle_x + \langle \delta d\theta_u, \delta d\theta_u \rangle_x dV = \int_\Omega \langle \Delta\theta_u, \Delta\theta_u \rangle_x dV = \sum_i \frac{\lambda_i^2}{(1-\lambda_i)^2} a_i^2 \leq \sum_i |a_i|^2. \tag{64}
$$

This shows that $(1 - \Delta)^{-1}\mu$ is a well-defined twice-differentiable $1-$form.

B Proof of theorem 2.2

First assume that the manifold has C^1-boundary. Then the boundary condition v can be extended to $u_0 \in H^1(\Omega)$ such that $u_0\big|_{\partial\Omega} = v$. Thus the optimisation problem (40) is equivalent to

$$\begin{cases} u(t) = \underset{u \in H^1(T\Omega)}{\arg\min} \displaystyle\int_\Omega |\theta_t + \mathcal{L}_{u_0}\theta + \mathcal{L}_u\theta|_x^2 + |d\theta_u + d\theta_{u_0}|_x^2 + |\delta\theta_u + \delta\theta_{u_0}|_x^2 \\ u(t)\big|_{\partial\Omega} = 0. \end{cases} \tag{65}$$

The first term in the above functional can be rewritten as

$$\langle \mathcal{L}_u\theta, \mathcal{L}_u\theta\rangle_x + 2\langle \mathcal{L}_u\theta, \theta_t + \mathcal{L}_{u_0}\theta\rangle_x + |\theta_t + \mathcal{L}_{u_0}\theta|_x^2 \tag{66}$$

Since $\theta \in H^1, u_0 \in H^1$, $\mathcal{L}_{u_0}\theta \in L^2$. Note that for the space of vector fields vanishing on $\partial\Omega$, the L^2 norm of u is bounded by $|d\theta_u|^2 + |\delta\theta_u|^2$ up to a constant depending on the domain only. For u, w of finite H^1 norm and vanishing on the boundary, let

$$B(u, w) = \int_\Omega \langle \mathcal{L}_u\theta, \mathcal{L}_w\theta\rangle_x + \langle d\theta_u, d\theta_w\rangle_x + \langle \delta\theta_u, \delta\theta_w\rangle_x dV \tag{67}$$

$$a(u) = \int_\Omega \langle \mathcal{L}_u\theta, \theta_t + \mathcal{L}_{u_0}\theta\rangle_x dV \tag{68}$$

Obviously B is symmetric and coercive due to Poincare lemma. We will show that B is bounded and a is continuous with respect to the H^1 norm. Then B gives an equivalent norm as the common H^1 norm, denoted by $\|\cdot\|_B$. Then by Riesz representation theorem, there exists $f \in H^1(T\Omega)$ which vanishes on $\partial\Omega$, such that $a(u) = \langle u, f\rangle_B$. Then

$$B(u, u) + a(u) = \langle u, u\rangle_B + 2\langle u, f\rangle_B \geq \langle u + f, u + f\rangle_B - \|f\|_B^2, \tag{69}$$

implying that $-f$ is the unique solution. Next we show that B and a are continuous forms.

For the continuity of a, following a similar argument as those in appendix A, there exists finitely many $\eta_i \in H^1(T^*\Omega)$ with bounded $|d\eta_i|_x$ and $\xi_i \in L^2(T^*\Omega)$ depending only on the given data, such that

$$a(u) = \sum_i \int_\Omega \langle \mathcal{L}_u\eta_i, \xi_i\rangle_x dV \tag{70}$$

We can further assume that η_i, ξ_i are compactly supported inside a local coordinate (Ω_i, x). Since $|d\eta_i|_x$ is bounded,

$$\|\mathcal{L}_u\eta_i\|_{L^2} = \|d\iota_u\eta_i + \iota_u d\eta_i\|_{L^2} = \|d(\eta_i(u)) + \iota_u d\eta_i\|_{L^2} \lesssim \|u\|_{H^1}. \tag{71}$$

Thus

$$|a(u)| \lesssim \sum_i \|\mathcal{L}_u\eta_i\|_{L^2}\|\xi_i\|_{L^2} \lesssim \|u\|_{H^1}. \tag{72}$$

In order to show that B is bounded, following the same argument in appendix A, there exists finitely many differential 1-forms η_i in H^1 with bounded $|d\eta_i|_x$, and bounded functions m_i, such that

$$\langle \mathcal{L}_u\theta, \mathcal{L}_u\theta\rangle_x = \sum_i m_i \langle \mathcal{L}_u\eta_i, \mathcal{L}_u\eta_i\rangle_x. \tag{73}$$

Therefore $\|\mathcal{L}_u\theta\|_{L^2}^2 \lesssim \|u\|_{H^1}^2$, meaning that B is bounded. The proof for the case when Ω is a compact oriented Riemannian manifold without boundary is similar, thus omitted.

C Details of the numerical experiments

C.1 Model and domain

The data assimilation experiment is conducted using the thermal shallow water equation [27]. This model consists of three state variables: $h-$the water height, $v = (v^1, v^2)-$the velocity field, and $\Theta-$the buoyancy (or density contrast):

$$\frac{\partial h}{\partial t} + \nabla \cdot (hv) = 0, \tag{74}$$

$$\frac{\partial \Theta}{\partial t} + (v \cdot \nabla)\Theta = -\kappa(h\Theta - h_0\Theta_0), \tag{75}$$

$$\frac{\partial v}{\partial t} + (v \cdot \nabla)v + f\hat{z} \times v = -\nabla(h\Theta) + \frac{1}{2}h\nabla\Theta. \tag{76}$$

Both Θ and h are assumed strictly positive at each point.

The quantity h follows a dynamics similar to the state variable S in example 2.2.2, and transportation terms for Θ follow those in example 2.2.1. A natural choice is then $\theta_h = h dx^1 \wedge dx^2$, a differential 2-form, and $\theta_\Theta = \Theta$ a differential 0-form. The test case is a double-vortex case. Hence $\theta_v = v^1 dx^1 + v^2 dx^2$ is chosen to ensure vorticity conservation during the morphing process. These choices of differential forms differ from those presented in [30]. Less constrained by the underlying dynamics, [30] discussed the derivation of a perturbation scheme able to conserve particular quantities. Here, the choice for the tensor fields should obey to the prescribed dynamics of the system to maximally maintain the dynamical balance during the morphing process.

The data assimilation process is solely conducted for one time step. It is assumed that both the vorticity field $\omega = \frac{\partial v^2}{\partial x^1} - \frac{\partial v^1}{\partial x^2}$ and the h field are fully observed. Since $\theta_v = v^1 dx^1 + v^2 dx^2$, naturally ω is associated to a differential 2-form $\theta_\omega = \omega dx^1 \wedge dx^2 = d\theta_v$.

The domain is 2-dimensional doubly periodic: $\Omega = [0, 5000\text{km}]_{\text{per}} \times [0, 5000\text{km}]_{\text{per}}$, which is a compact Riemannian manifold without boundary. In this case, a numerical solution of (14), or equivalently the numerical solution of Eq.(62), with $a = 1$, can be derived in the Fourier space. In fact, the vector field u is separately calculated for h observations and for ω observations. From the two observables, the explicit expressions of u are:

$$u_\omega = (u^1_\omega, u^2_\omega) = 2(I - \Delta)^{-1}\big[\omega_2 \nabla(\omega_1 - \omega_2)\big], \tag{77}$$

$$u_h = (u^1_h, u^2_h) = 2(I - \Delta)^{-1}\big[h_2 \nabla(h_1 - h_2)\big]. \tag{78}$$

The final u for each iterative step is then chosen to be $\frac{1}{2}(\frac{u_\omega}{\|u_\omega\|_1} + \frac{u_h}{\|u_h\|_1})$, in which

$$\|u\|_1^2 = \int_\Omega \langle\theta_u, \theta_u\rangle_x + \langle d\theta_u, d\theta_u\rangle_x + \langle\delta\theta_u, \delta\theta_u\rangle_x dV = \int_\Omega |u|^2 + |\nabla u^1|^2 + |\nabla u^2|^2 dx^1 dx^2. \tag{79}$$

C.2 Numerical methods and experimental parameters

The units in the code are set to be km and 100s. The initial condition and model parameters are taken from the numerical experiment in subsection (5.3) of [10]. The 3-step Adams-Bashforth method (see for instance chapter 3.1 of [11]) is used in model integration. Additionally, the one dimensional Hou-Li spectral filter [12] $\exp\{-36[(k_x/k_{max})^a + (k_y/k_{max})^a]\}$, with $a = 12$, is applied to the Fourier modes of the state vector at the end of each model integration step. The truth is generated by running the model forward for 2750 time units. To generate the ensemble members, the center of the initial vortex, (ox, oy), is perturbed:

$$ox \sim \mathcal{N}(0.1, 0.01), \quad oy \sim \mathcal{N}(0.1, 0.01). \tag{80}$$

The ensemble members are then generated by running the model forward starting from perturbed initial condition for 2000 time units. For the explicit meaning of ox and oy, please refer to section 5.3 of [10]. The ensemble size $N_e = 20$. Both the ensemble members and the truth are generated using a 256×256 grid. But before starting the morphing process or data assimilation, the ensemble members and the observations are both projected to a coarse-grid (64×64) and then interpolated back to the original grid (256×256).

The morphing process is implemented with the 5-step Adams-Bashforth method and the spectral Hou-Li filter with $a = 36$. For clarity, the pseudo-code of the complete morphing process is shown in Algorithm 2. We choose $\epsilon = 0.000033$ and $N = 10000$.

The observation is exactly the same as the interpolated value of the truth. There is no error in the observation. However, the matrix R in ensemble Kalman filter is set to be a diagonal matrix with diagonal elements equal to

$$R_\omega = \frac{0.01}{64^2} \sum_{i=1}^{64^2} (\omega_i^{\text{obs}})^2, \text{ or } R_h = \frac{0.01}{64^2} \sum_{i=1}^{64^2} (h_i^{\text{obs}})^2, \tag{81}$$

where ω_i^{obs} and h_i^{obs} refer to the ω value and h value at the $i-$th grid-point in the 64×64 grid. Data assimilation is conducted on the 64×64 grid.

References

[1] Determining optical flow. Artificial Interlligence, 17:185–203.

[2] J. D. Beezley and J. Mandel. Morphing ensemble kalman filters. Tellus A: Dyn. Meteorol. Oceanogr., 60:131 – 140, 2007.

Algorithm 2: The pseudo-code for the nudging process with Adams-Bashforth method for thermal shallow water model on a doubly periodic domain.

Data: ω^{true}, h^{true}, h^{model}, v^{model}, and Θ^{model} on a 256×256 grid of Ω; small positive number $\epsilon > 0$; the total number of iterations N.
Result: morphed model estimates h^{morphed}, Θ^{morphed}, and v^{morphed}.

$\omega_1 \leftarrow \omega^{\text{true}}$; $h_1 \leftarrow h^{\text{true}}$; $h_2 \leftarrow h^{\text{model}}$; $\Theta_2 \leftarrow \Theta^{\text{model}}$; $v_2 \leftarrow v^{\text{model}}$; $\omega_2 \leftarrow \dfrac{\partial v_2^2}{\partial x^1} - \dfrac{\partial v_2^1}{\partial x^2}$;

Set $\mathtt{d}h, \mathtt{d}h_{-1}, \mathtt{d}h_{-2}, \mathtt{d}h_{-3}, \mathtt{d}h_{-4}, \mathtt{d}\Theta, \mathtt{d}\Theta_{-1}, \mathtt{d}\Theta_{-2}, \mathtt{d}\Theta_{-3}, \mathtt{d}\Theta_{-4}, \mathtt{d}v, \mathtt{d}v_{-1}, \mathtt{d}v_{-2}, \mathtt{d}v_{-3}, \mathtt{d}v_{-4}$ all as 0 arrays of the proper sizes ;

for $i = 1, 2, ..., N$ **do**

- Calculate u_ω using Eq.(77);
- Calculate u_h using Eq.(78);
- $u_i \leftarrow \frac{1}{2}(\frac{u_\omega}{\|u_\omega\|_1} + \frac{u_h}{\|u_h\|_1})$;
- $\mathtt{d}h_{-4} \leftarrow \mathtt{d}h_{-3}$, $\mathtt{d}h_{-3} \leftarrow \mathtt{d}h_{-2}$, $\mathtt{d}h_{-2} \leftarrow \mathtt{d}h_{-1}$, $\mathtt{d}h_{-1} \leftarrow \mathtt{d}h$, do the same for $\mathtt{d}\Theta$ and $\mathtt{d}v$;
- $\mathtt{d}h \leftarrow \nabla \cdot (h_2 u_i),\ \mathtt{d}\Theta \leftarrow u_i \cdot \nabla\Theta_2,\ \mathtt{d}v = (v_2 \cdot \dfrac{\partial u_i}{\partial x^2} + u_i \cdot \nabla v_2^1, v_2 \cdot \dfrac{\partial u_i}{\partial x^2} + u_i \cdot \nabla v_2^2)$;
- $h_2 \leftarrow h_2 + \epsilon(\frac{1901}{720}\mathtt{d}h - \frac{2774}{720}\mathtt{d}h_{-1} + \frac{2616}{720}\mathtt{d}h_{-2} - \frac{1274}{720}\mathtt{d}h_{-3} + \frac{251}{720}\mathtt{d}h_{-4})$, do the same for Θ_2 and v_2;
- Apply the spectral Hou-Li filter to h_2, Θ_2, and v_2;
- $\omega_2 \leftarrow \dfrac{\partial v_2^2}{\partial x^1} - \dfrac{\partial v_2^1}{\partial x^2}$;

end

$h^{\text{morphed}} \leftarrow h_2$, $\Theta^{\text{morphed}} \leftarrow \Theta_2$, $v^{\text{morphed}} \leftarrow v_2$

[3] M. F. Beg, M. I. Miller, A. Trouvé, and L. Younes. Computing large deformation metric mappings via geodesic flows of diffeomorphisms. Int. J. Comput. Vision, 61:139–157, 2005.

[4] M. Bruveris, F. Gay-Balmaz, D. D. Holm, and T. S. Ratiu. The momentum map representation of images. J. Nonlinear Sci., 21:115–150, 2009.

[5] T. Corpetti, É. Mémin, and P. Pérez. Dense estimation of fluid flows. IEEE Trans. Pattern Anal. Mach. Intell., 24:365–380, 2002.

[6] P. Courtier, J.-N. Thépaut, and A. Hollingsworth. A strategy for operational implementation of 4d-var, using an incremental approach. Q. J. R. Meteorolog. Soc., 120(519):1367–1387, 1994.

[7] P. Del Moral. Nonlinear filtering: Interacting particle resolution. Comptes Rendus de l'Académie des Sciences - Series I - Mathematics, 325(6):653–658, 1997.

[8] P. Dérian, P. Héas, C. Herzet, and É. Mémin. Wavelets and optical flow motion estimation. Numer. Math. theory Methods Appl., 6:116–137, 2013.

[9] G. F. D. Duff and D. C. Spencer. Harmonic tensors on riemannian manifolds with boundary. Ann. Math., 56:128, 1952.

[10] C. Eldred, T. Dubos, and E. Kritsikis. A quasi-hamiltonian discretization of the thermal shallow water equations. J. Comput. Phys., 379:1–31, 2019.

[11] E. Hairer, G. Wanner, and S. P. Nørsett. Solving Ordinary Differential Equations I. Springer series in computational mathematics. Springer Berlin, Heidelberg, 1993.

[12] T. Y. Hou and R. Li. Computing nearly singular solutions using pseudo-spectral methods. J. Comput. Phys., 226:379–397, 2007.

[13] P. Houtekamer and H. L. Mitchell. A sequential ensemble kalman filter for atmospheric data assimilation. Mon. Wather Rev., 129:123–137, 2001.

[14] P. L. Houtekamer and H. L. Mitchell. Data assimilation using an ensemble Kalman filter technique. Mon. Wather Rev., 126(3):796–811, 1998.

[15] R. E. Kalman. A New Approach to Linear Filtering and Prediction Problems. Journal of Basic Engineering, 82(1):35–45, 03 1960.

[16] J. Lefévre and S. Baillet. Optical flow and advection on 2-riemannian manifolds: A common framework. IEEE Trans. Pattern Anal. Mach. Intell., 30:1081–1092, 2008.

[17] A. C. Lorenc. Analysis methods for numerical weather prediction. Quarterly Journal of the Royal Meteorological Society, 112:1177–1194, 1986.

[18] E. Meinhardt, J. S. Pérez, and D. Kondermann. Horn-schunck optical flow with a multi-scale strategy. Image Process. Line, 3:151–172, 2013.

[19] E. Ott and B. R. Hunt. A local ensemble Kalman filter for atmospheric data assimilation. Tellus, 56A:415–428, 2004.

[20] S. C. Ravela, K. A. Emanuel, and D. B. McLaughlin. Data assimilation by field alignment. Physica D, 230:127–145, 2007.

[21] S. Rosenberg. The Laplacian on a Riemannian Manifold: An Introduction to Analysis on Manifolds. London Mathematical Society Student Texts. Cambridge University Press, 1997.

[22] G. Schwarz. Hodge Decomposition - A Method for Solving Boundary Value Problems. Springer Berlin, Heidelberg, 1995.

[23] A. Trouvé. Diffeomorphisms groups and pattern matching in image analysis. International Journal of Computer Vision, 28:213–221, 1998.

[24] A. Trouvé and L. Younes. Local geometry of deformable templates. SIAM J. Math. Anal., 37:17–59, 2005.

[25] A. Trouvé and L. Younes. Metamorphoses through lie group action. Found. Comput. Math., 5:173–198, 2005.

[26] A. Trouvé. An infinite dimensional group approach for physics based models in pattern recognition. International Journal of Computer Vision - IJCV, 01 1995.

[27] E. S. Warneford and P. J. Dellar. The quasi-geostrophic theory of the thermal shallow water equations. J. Fluid Mech., 723:374 – 403, 2013.

[28] R. P. Wildes, M. J. Amabile, A.-M. Lanzillotto, and T.-S. Leu. Recovering estimates of fluid flow from image sequence data. Comput. Vis. Image Underst., 80:246–266, 2000.

[29] L. Younes, I. Herlin, and D. Béréziat. A generalized optical flow constraint and its physical interpretation. In Proceedings IEEE Conference on Computer Vision and Pattern Recognition. CVPR 2000, volume 3, page 2487, Los Alamitos, CA, USA, jun 2000. IEEE Computer Society.

[30] Y. Zhen, V. Resseguier, and B. Chapron. Physically constrained covariance inflation from location uncertainty. Nonlinear Process. Geophys., 2023.